Supporting Information

Surfactant-directed syntheses of mesostructured zinc imidazolates: Formation mechanism and structural insights

Erik A. Flügel,[abc] Matthew T. Aronson,[d] Sebastian C. Junggeburth,[abc] Bradley F. Chmelka,[d] and Bettina V. Lotsch[abc]

[a]Max Planck Institue for Solid State Research, Stuttgart, Germany
[b]Ludwig Maximilian University (LMU), Department of Chemistry, Munich, Germany
[c]Nanosystems Initiative Munich (NIM) & Center for Nanoscience (CeNS), Munich, Germany
[d]Department of Chemical Engineering, University of California, Santa Barbara, California, U.S.A.

Table S1: Chemicals used in this work and their respective suppliers and purity.

Chemical name	**Supplier**	**Purity**
Zinc acetate dihydrate	Merck	ACS
Imidazole	Acros Organics	99 %
2-Methylimidazole	Merck	99 %
N,N-dimethyltetradecylamine	Sigma Aldrich	≥ 95 %
N,N-dimethylhexadecylamine	Sigma Aldrich	≥ 95 %
N,N-dimethyloctadecylamine	Sigma Aldrich	≥ 95 %
1,4-dibromobutane	Alfa Aesar	99 %
1,5-dibromopentane	Alfa Aesar	98 %
1,6-dibromohexane	Alfa Aesar	96 %
1,7-dibromoheptane	Acros Organics	97 %
1,8-dibromooctane	Acros Organics	98 %
1,9-dibrononane	Acros Organics	97 %
1,10-dibromodecane	Acros Organics	97 %
Cetyltrimethylammoniumbromide (CTAB)	Alfa Aesar	98 %
n-heptane	Sigma Aldrich	99 %
1-hexanol	Alfa Aesar	99 %
THF	Chemetall	99.9 %
Diethylether	VWR	99.7 %
2-propanol	Sigma Aldrich	99.5 %
Dioxan	Sigma Aldrich	≥ 99 %
Ehtylacetate	VWR	99 %
Methanol	Sigma Aldrich	99.9 %
Ethanol	Bundesmonopolverwaltung für Brandwein	99.8 %
Acetone	Sigma Aldrich	≥ 99 %

Table S2: *d*-spacings of the first observable stacking reflections in the powder XRD measurements of all as-made MIF materials synthesized with 16-10-16 gemini surfactants, as a function of the solvent used.

Solvent	IM MIF	MeIM MIF
Microemulsion (n-heptane/1-hexanol)	33.2	33.0
THF	33.5	32.8
Diethylether	34.0	32.7
2-Propanol	33.1	32.6
Dioxan	33.4	32.4
Ethylacetate	34.0	32.4
Ethanol	33.4	32.4
Methanol	33.4	32.4
Acetone	32.9	32.2

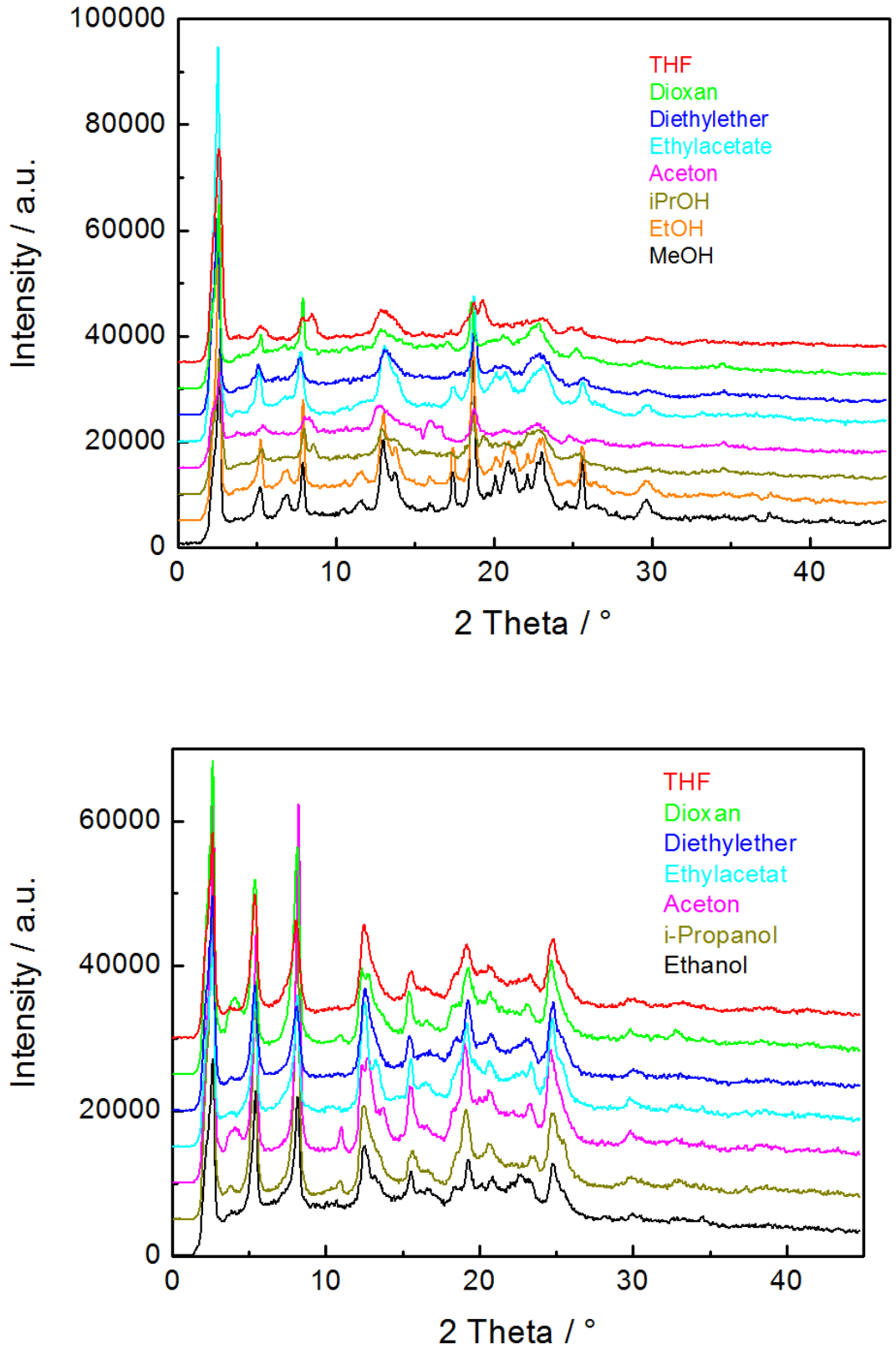

Figure S1: Powder XRD patterns obtained for IM MIF (top) and MeIM MIF (bottom) synthesized with 16-10-16 gemini surfactants in various solvents.

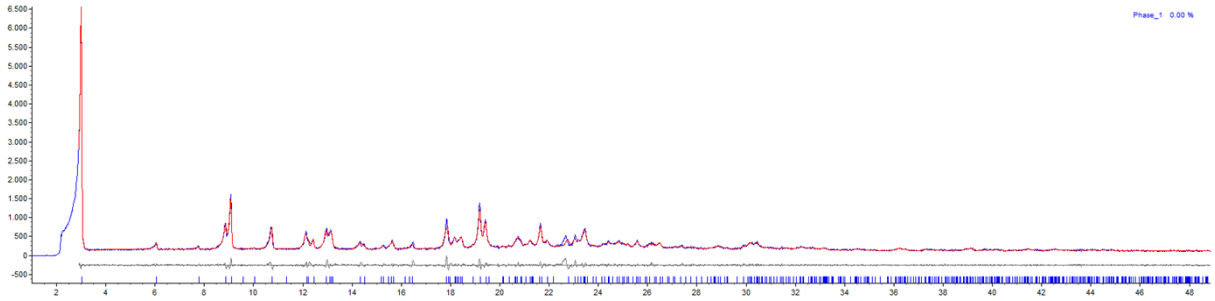

Figure S2: Pawley fit for IM MIF (*C*2, a = 11.5829 Å, b = 58.253 Å, c = 9.2415 Å, β = 88.94°, wR = 7.57, GoF = 1.286) synthesized with 16-8-16 gemini surfactants.

Table S3: Percent elemental compositions from bulk elemental analyses of various MIF compounds and comparisons with the expected values for stoichiometric compositions of the hybrid materials with 1 zinc : 1 IM/MeIM : 2 bromine : 0.5 surfactant.

14-6-14, Im, MIF	**Zn**	**C**	**N**	**H**	**Br**
Measured values	8.0	55.9	6.9	9.9	19.3
Expected values	7.9	56.5	6.8	9.6	19.3
Difference	0.1	-0.6	0.1	0.3	0.0

16-10-16, Im, MIF	**Zn**	**C**	**N**	**H**	**Br**
Measured values	6.6	60.4	5.8	10.3	16.7
Expected values	7.0	59.9	6.0	10.2	17.0
Difference	-0.4	0.5	-0.2	0.1	-0.3

18-10-18, Im MIF	**Zn**	**C**	**N**	**H**	**Br**
Measured values	6.7	61.6	5.6	9.9	16.2
Expected values	6.6	61.4	5.6	10.4	16.0
Difference	0.1	0.2	0.0	-0.5	0.2

14-6-14, 2MIm, MIF	**Zn**	**C**	**N**	**H**	**Br**
Measured values	7.5	57.3	6.5	9.6	18.8
Expected values	7.8	57.0	6.6	9.7	19.0
Difference	-0.3	0.3	-0.1	-0.1	-0.2

16-10-16, 2MIm, MIF	**Zn**	**C**	**N**	**H**	**Br**
Measured values	6.9	59.9	6.0	10.1	17.0
Expected values	6.9	60.4	5.9	10.2	16.7
Difference	0.0	-0.5	0.1	-0.1	0.3

18-10-18, 2MIm MIF	**Zn**	**C**	**N**	**H**	**Br**
Measured values	6.5	61.7	5.5	10.6	15.7
Expected values	6.5	61.7	5.5	10.5	15.8
Difference	0.0	0.0	0.0	0.1	-0.1

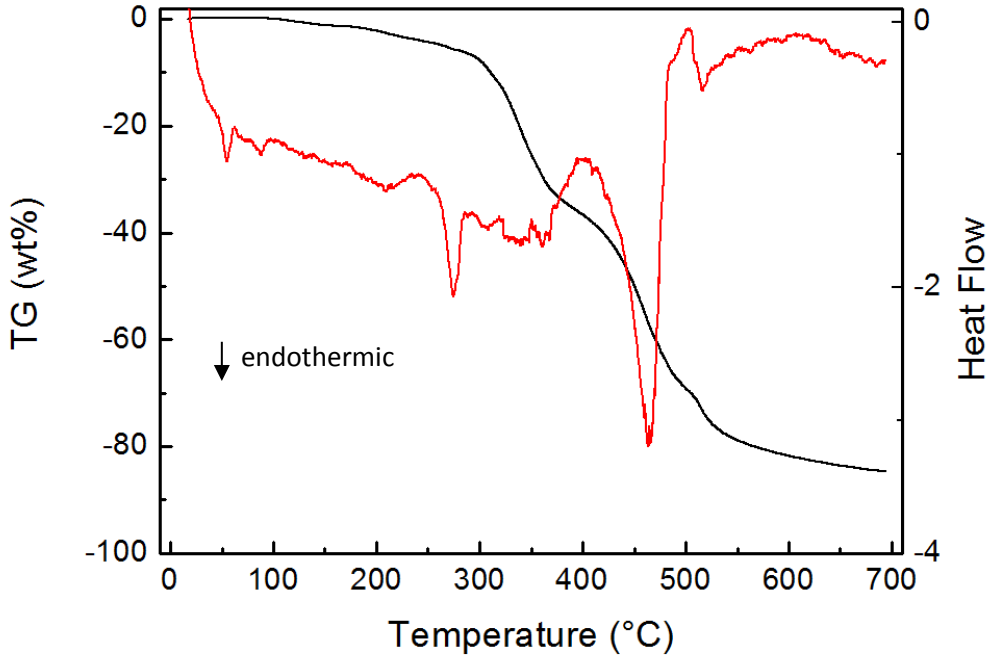

Figure S3: DTA/TG curves of 16-10-16 MeIM bridged MIF, suggesting thermal stability up to 300°C. The endothermic heat flow below 300 °C likely reflects thermally activated rearrangements and quasi-melting of the surfactants in the hybrid material.

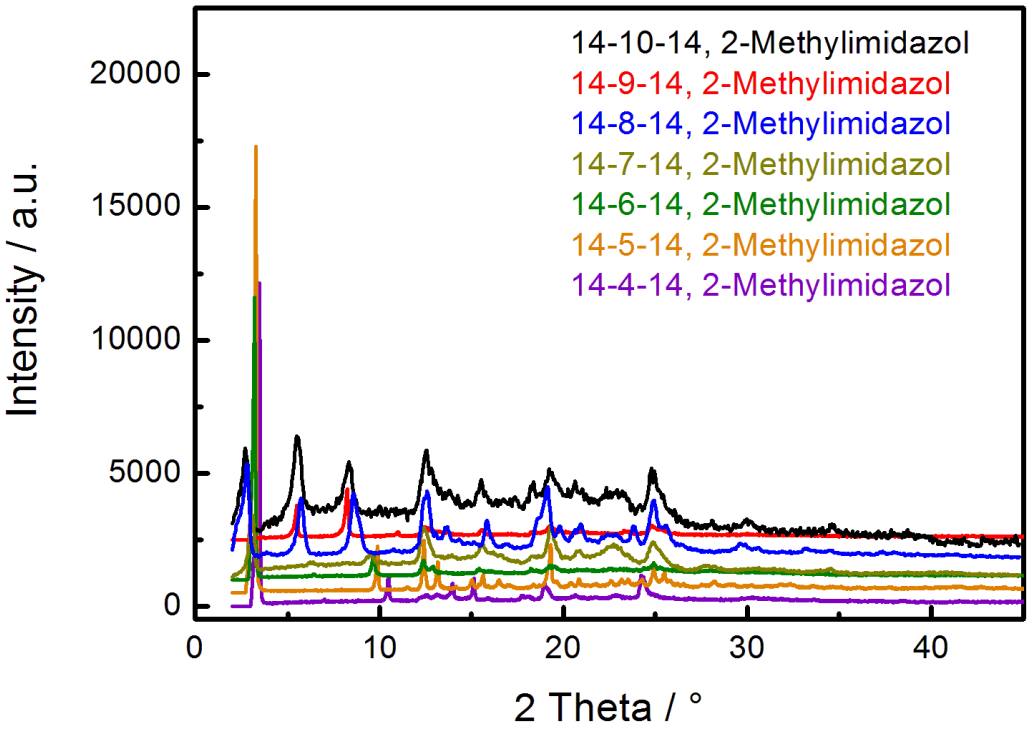
14-10-14, 2-Methylimidazol
14-9-14, 2-Methylimidazol
14-8-14, 2-Methylimidazol
14-7-14, 2-Methylimidazol
14-6-14, 2-Methylimidazol
14-5-14, 2-Methylimidazol
14-4-14, 2-Methylimidazol
Intensity / a.u.
20000
15000
10000
5000
0
0
10
20
30
40
2 Theta / °

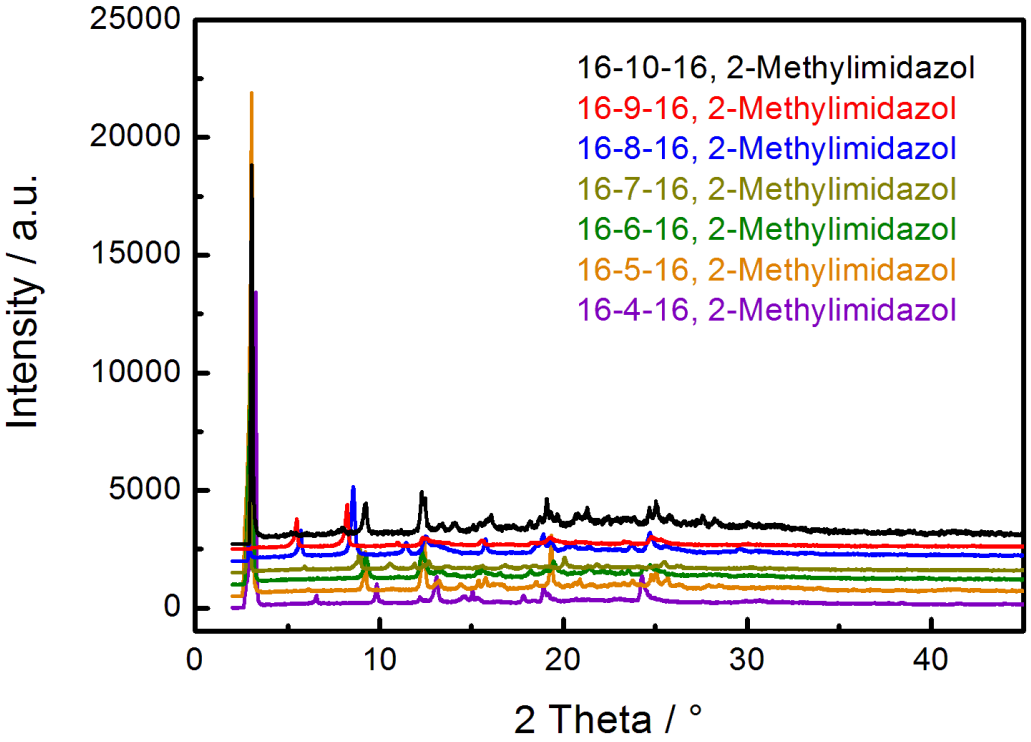
16-10-16, 2-Methylimidazol
16-9-16, 2-Methylimidazol
16-8-16, 2-Methylimidazol
16-7-16, 2-Methylimidazol
16-6-16, 2-Methylimidazol
16-5-16, 2-Methylimidazol
16-4-16, 2-Methylimidazol
Intensity / a.u.
25000
20000
15000
10000
5000
0
0
10
20
30
40
2 Theta / °

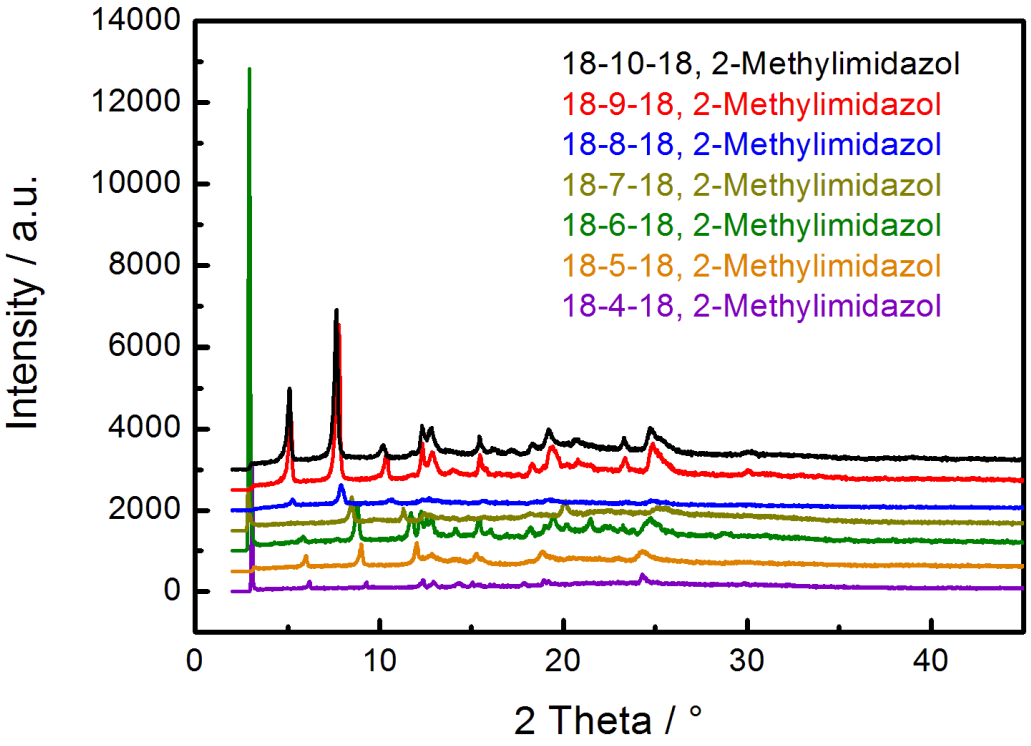
Intensity / a.u.
14000
12000
10000
8000
6000
4000
2000
0
0
10
20
30
40
2 Theta / °
18-10-18, 2-Methylimidazol
18-9-18, 2-Methylimidazol
18-8-18, 2-Methylimidazol
18-7-18, 2-Methylimidazol
18-6-18, 2-Methylimidazol
18-5-18, 2-Methylimidazol
18-4-18, 2-Methylimidazol

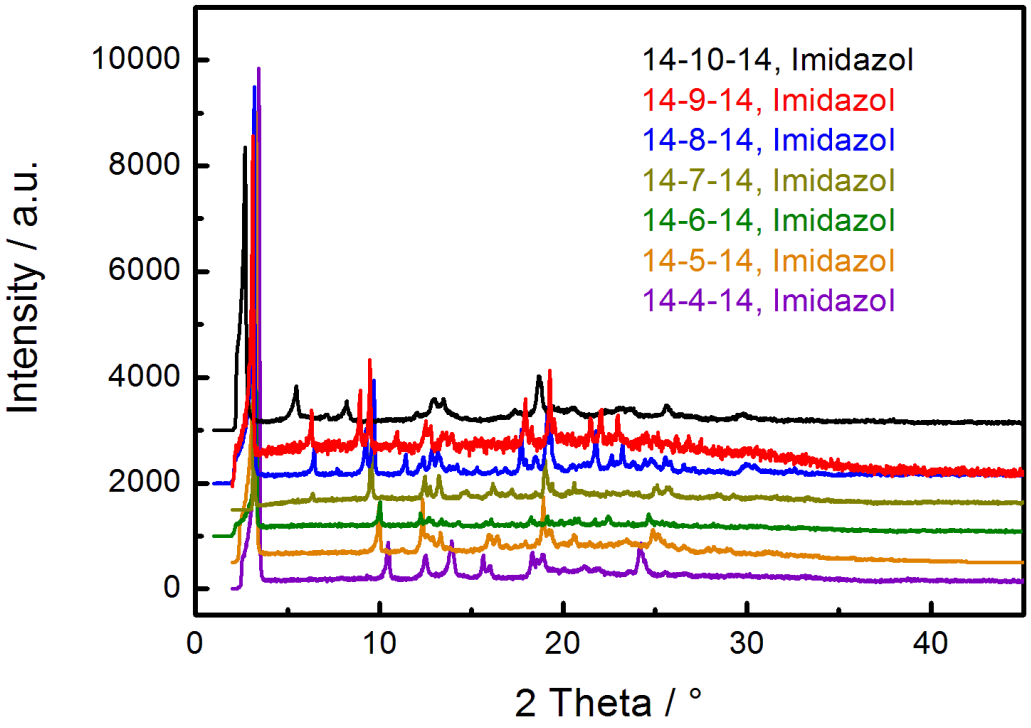
Intensity / a.u.
10000
8000
6000
4000
2000
0
0
10
20
30
40
2 Theta / °
14-10-14, Imidazol
14-9-14, Imidazol
14-8-14, Imidazol
14-7-14, Imidazol
14-6-14, Imidazol
14-5-14, Imidazol
14-4-14, Imidazol

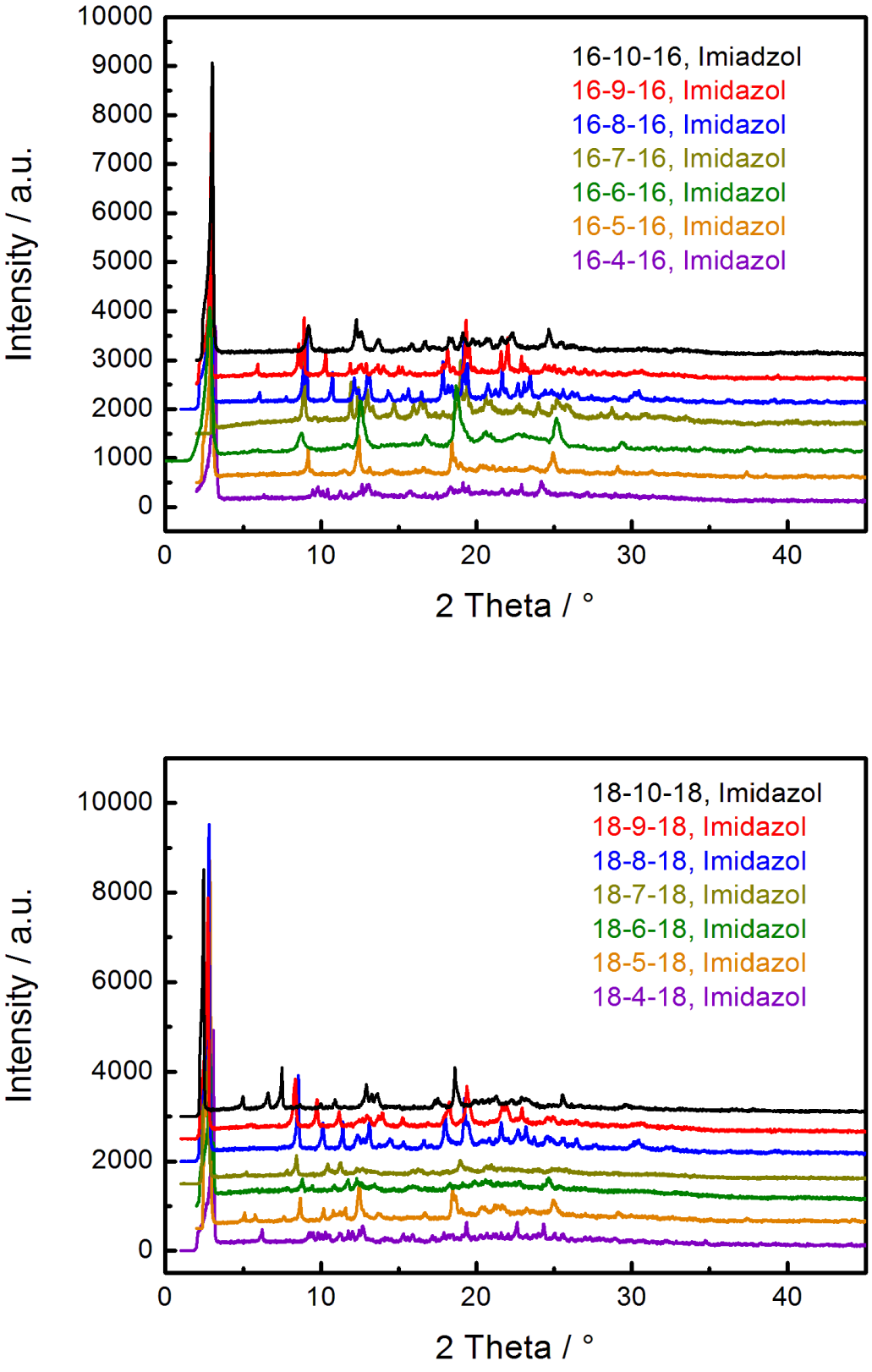

Figure S4: Powder XRD patterns of MeIM- and IM-bridged MIFs synthesized with different gemini surfactants. From top to bottom: 14-*m*-14 MeIM, 16-*m*-16 MeIM, 18-*m*-18 MeIM, 14-*m*-14 IM, 16-*m*-16 IM, 18-*m*-18 IM.

Table S4: *d*-spacings of the first observable stacking reflections in the powder XRD measurements of all as-synthesized MIF materials.

Tail Length	Spacer Length	IM MIF	MeIM MIF
14	**4**	25.4	25.3
14	**5**	26.8	26.9
14	**6**	26.6	27.5
14	**7**	27.6	28.1
14	**8**	27.5	29.5
14	**9**	28.2	30.4
14	**10**	32.6	31

Tail Length	Spacer Length	IM MIF	MeIM MIF
16	**4**	28.1	27.0
16	**5**	29.1	28.8
16	**6**	28.9	28.7
16	**7**	29.5	29.7
16	**8**	29.4	31.0
16	**9**	30.0	32.3
16	**10**	33.2	33.0

Tail Length	Spacer Length	IM MIF	MeIM MIF
18	**4**	28.6	28.6
18	**5**	30.7	29.4
18	**6**	30.4	30.2
18	**7**	31.8	31.2
18	**8**	31.4	33.6
18	**9**	32.1	34.1
18	**10**	35.7	34.7

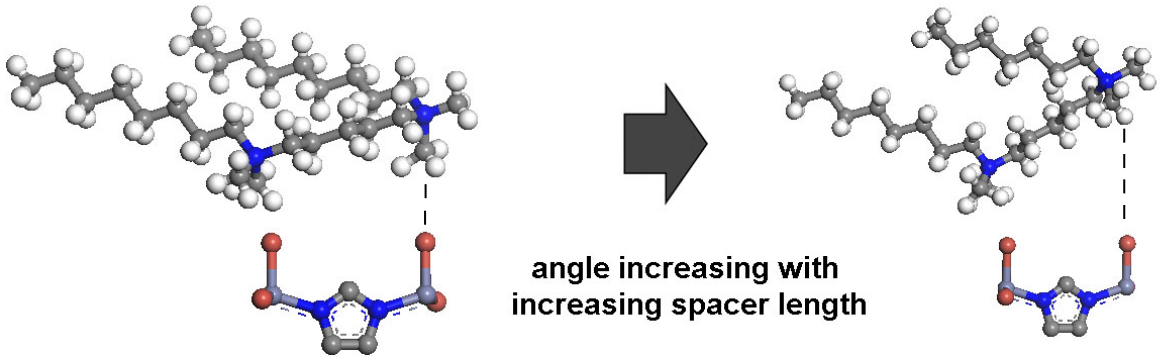

Figure S5: Proposed charge compensation by geometric rearrangement of the surfactant headgroups to comply with the charge density of the inorganic slabs. The angle between surfactant spacer and zinc imidazolate chains increases with growing spacer length. To simplify this image, only a single $[ZnIMBr_2]^-$ unit is shown and the carbon tail-groups (*m*) of the surfactants have been shortened.

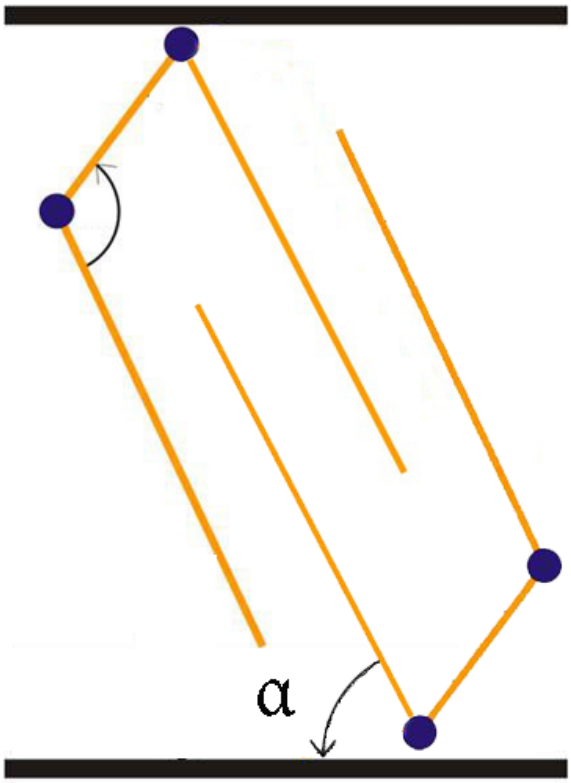

Figure S6: Schematic diagram depicting the proposed tilted interdigitated, anti-parallel arrangement of the surfactant in the as-synthesized MIF materials, showing the angle α between the tail groups and the zinc imidazolate layers.

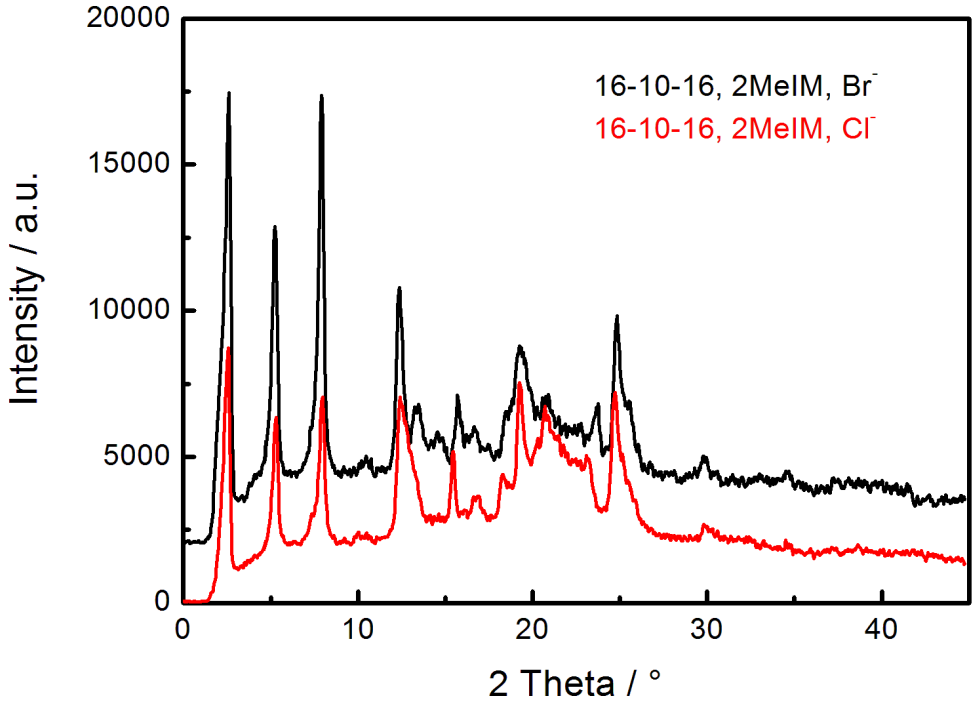

Figure S7: Powder XRD patterns of MeIM-bridged MIFs synthesized in the presence of different halogenide ions.

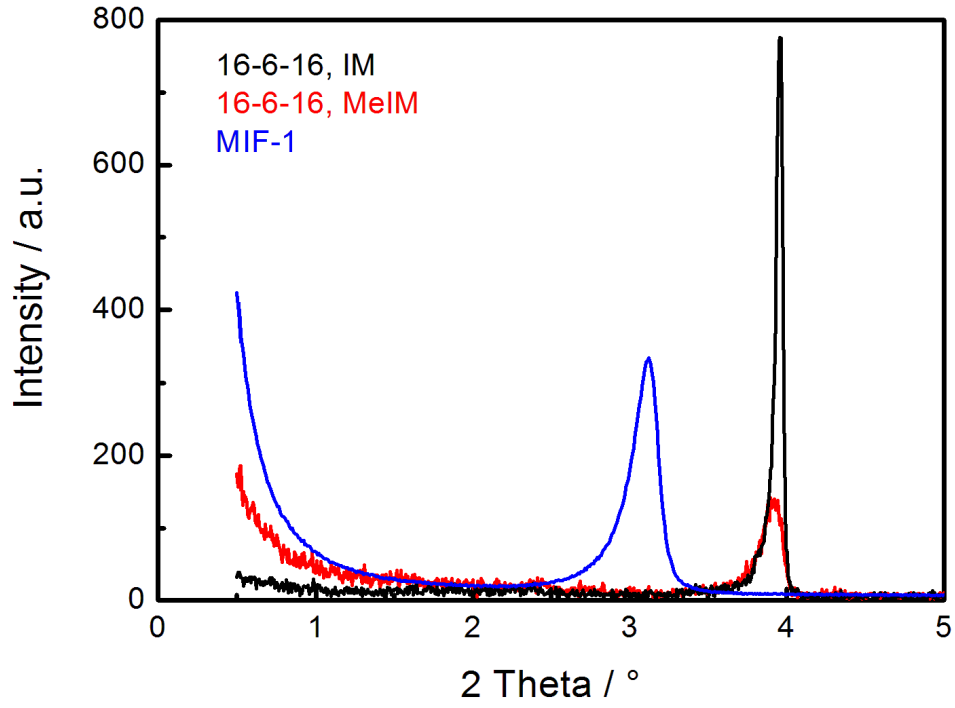

Figure S8: Small-angle XRD patterns of gemini-directed materials and MIF-1 showing the first reflections corresponding to the lamellar stacking of the as-synthesized materials.

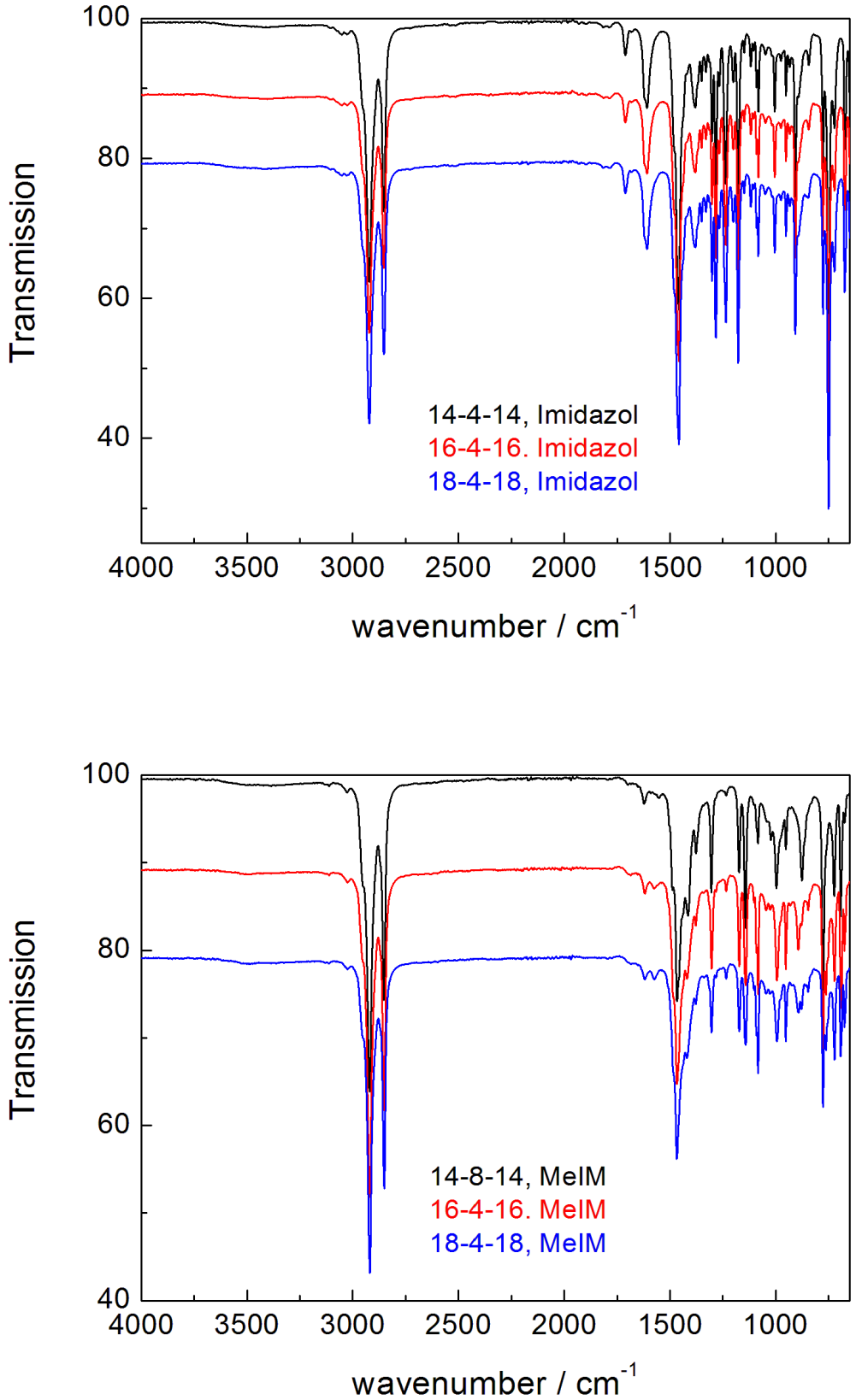

Figure S9: Infrared spectra showcasing the similarity between the MeIM/IM MIFs templated by different gemini-surfactants.

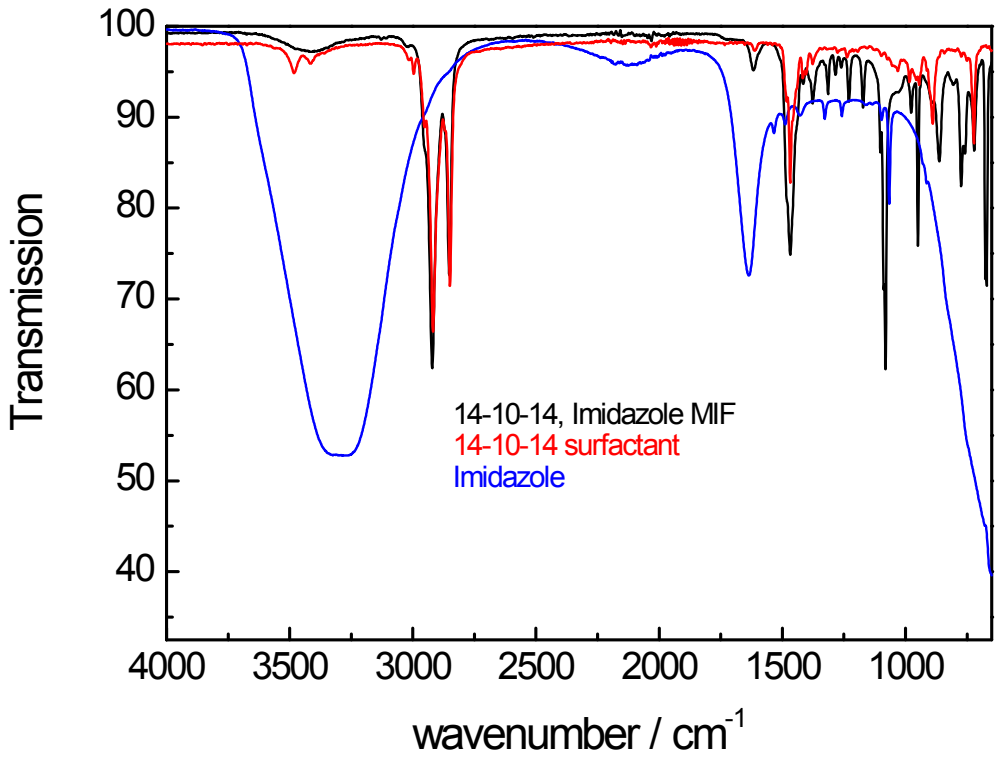

Figure S10: Infrared spectra showcasing the similarities and purity of the synthesized MIF materials in comparison to the starting materials used.

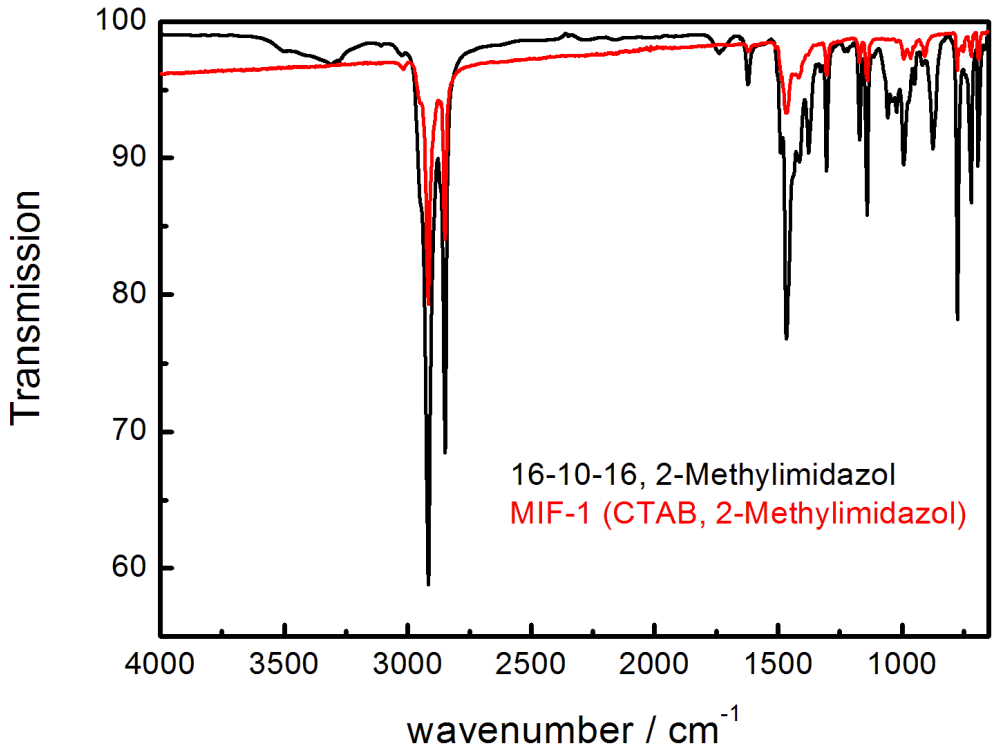

Figure S11. Infrared spectra showcasing the similarities between prototypic MIF-1 (CTAB/MeIM) and the MIF obtained from synthesis with 16-10-16 gemini surfactant.